

Molecular Modeling Study of Diltiazem Mimics at L-Type Calcium Channels

Klaus-Jürgen Schleifer^{1,2} and Edith Tot¹

Received March 15, 1999; accepted July 1, 1999

Purpose. A theoretical study was performed to generate a pharmacophore model for chemically diverse structures that specifically interact with the diltiazem binding site of L-type calcium channels.

Methods. Via molecular mechanics and quantum chemical methods solvation energies, logP values, conformational and electronic features of classical 1,5-benzothiazepin-4(5H)-one (BTZ, e.g., diltiazem), 1-benzazepin-2-one (BZ), pyrrolo[2,1-d][1,5]benzothiazepine, pyrrolo[2,1-c][1,4]benzothiazine, and benzobicyclo[2.2.2]octyl amines derivatives were determined. Furthermore, the molecular electrostatic potentials (MEPs) and common interaction fields derived from use of the GRID programme were compared.

Results. This yielded a pharmacophore model with three crucial pharmacophoric characteristics, (1) two aromatic ring systems in a distance of about 6.7 Å, (2) a basic side chain with pK_a in the physiological range, and (3) a 4'-methoxy moiety. In addition, a strong negative MEP in 4-position (carbonyl oxygen) and hydrophobic electron-rich features in the position equivalent to the sulphur atom of BTZ derivatives were explored to be favourable for receptor binding and calcium antagonistic effect. Moreover, the stabilizing effect of substituents in 3-position of BZs on the bioactive "M" twist-boat conformation of the heptagonal ring could be demonstrated by molecular dynamics simulations.

Conclusions. Based on these molecular descriptors, the quinazolinone derivative MCI-176 is predicted to be a potential ligand of the diltiazem binding site.

KEY WORDS: molecular modelling; calcium entry blocker; 1,5-benzothiazepin-4(5H)-one; quinazolinone; MCI-176; voltage-gated calcium channels.

INTRODUCTION

Calcium entry blockers, such as 1,4-dihydropyridines (DHPs, e.g., nifedipine), phenylalkylamines (PAAs, e.g., verapamil) and benzothiazepines (BTZs, e.g., diltiazem) inhibit the intracellularly directed calcium flux through L-type voltage-gated calcium channels (VGCCs) (1,2). This feature makes them indispensable in the therapy of cardiovascular diseases like hypertension or angina pectoris. Their molecular targets are distinct, but allosterically coupled, high-affinity binding sites on the α_1 -subunit of VGCCs where they induce stabilization of the inactivated-closed channel mode (3). While DHP and PAA binding sites, respectively, are only sensitive to structurally closely related congeners, a competitive character to the BTZ binding site is described for a multitude of chemically diverse compounds. Besides naturally occurring benzyloquinolines

(e.g., papaverine) (4) or aporphine derivatives like apomorphine (5–7), special effort was directed towards the synthesis of new ligands by structural variation of the benzothiazepine scaffold of diltiazem leading to sulphur-free benzazepines, pyrrolo-fused BTZ and benzothiazine derivatives. A further simplification of these heterocyclic compounds yielded the carbocyclic benzobicyclo[2.2.2]octyl amines that still produce full BTZ-like activity. Due to many cases of serious adverse effects that have been reported during the therapy with diltiazem, including cutaneous vasculitis (8), thrombocytopenia (9), heart block (10), parkinsonism (11) and even fatal renal and hepatic toxicity (12), the development of novel drugs with enhanced efficacy is justified.

In order to explore the critical determinants of BTZ-like derivatives that contribute to high-affinity binding with the binding site, a molecular modeling study will be presented describing the generation and detailed characterization of a BTZ pharmacophore model.

MATERIALS AND METHODS

Ligands

The X-ray structure of diltiazem hydrochloride (Fig. 1) was extracted from Cambridge Structural Database (13,14). To eliminate short atom-atom contacts and conformational distortions produced by intermolecular interactions in the crystal lattice, diltiazem was geometry optimized using 100 iterations of the steepest descent algorithm.

For construction of all 1,5-benzothiazepin-4(5H)-one (BTZ, Table I), 1-benzazepin-2-one (BZ, Table I) and pyrrolo[2,1-d][1,5]benzothiazepine derivatives (PBTZ, Table II) the "M" twist-boat conformation was fixed for the heptagonal rings (see Fig. 1), since this conformation is consistently found in all derivatives with a 3-substituent cis-oriented relative to the adjacent phenyl ring.

Pyrrolo[2,1-c][1,4]benzothiazines (P6Zs, Table II), benzobicyclo[2.2.2]octyl amines (BOAs, Table III) and the quinazolinone derivative MCI-176 were generated employing the BUILDER module of the SYBYL software package (21). All investigated compounds were considered in the protonated cationic form, because a pK_a of 7.7 was detected experimentally for diltiazem (22), and substitution of the basic amine against a neutral amide function decreases binding affinity of BZs by approximately two orders of magnitude (16).

Conformational Analysis

Applying the SEARCH option within SYBYL a systematic conformational search for low-energy conformations was performed. To avoid exclusion of potential conformations in this early stage, electrostatic interactions have been neglected (i.e., atomic charges were not considered). In addition, the general and the 1–4 vdW-factor were scaled down to 75% and the vdW radii of hydrogen atoms were set to 1.2 Å. Flexible bonds were fully rotated using rotational increments of 1° or 10°. Conformations with energy higher than 5 kcal/mol above the absolute energy minimum were discarded. Using the programme IXGROS (23) the remaining conformers were grouped into common families belonging to identical local minima. The lowest energy member of each family was subsequently energy

¹ Heinrich-Heine-Universität Düsseldorf, Institute for Pharmaceutical Chemistry, Universitätsstrasse 1, D-40225 Düsseldorf, Germany.

² To whom correspondence should be addressed. (e-mail: kjs@pharm.uni-duesseldorf.de)

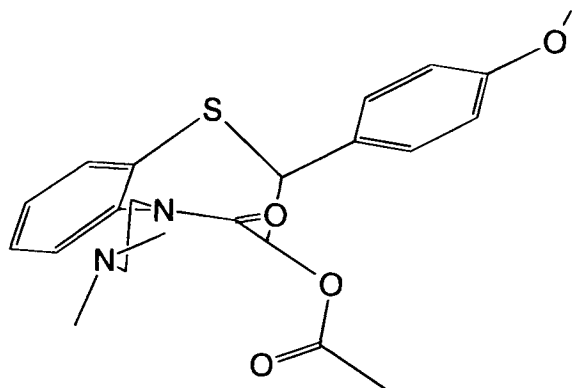


Fig. 1. X-ray structure of diltiazem hydrochloride (code CEYHUJ01) extracted from Cambridge Structural Database (13,14).

optimized applying the conjugate gradients algorithm until a maximum convergence criterion of 0.05 kcal/(mol · Å) was reached. Quality of the force field minimized derivatives was controlled via following semiempirical optimization applying the AM1 algorithm (24).

In order to investigate the conformational stability of the bioactive “M” twist-boat conformation of BZ derivatives, molecular dynamics simulations (mds) were performed within the TRIPOS force field (21) at temperatures of 310, 600, 700, 800 and 900 K for 500 ps taking snapshots of the actual conformer every 500 fs. Furthermore, the Merck Molecular Force Field (25) was applied to perform 10 cycles of a simulated annealing procedure with an initial temperature of 2000 K and a target temperature of 0 K. A period of 5 ps was chosen for both the high temperature and the annealing simulation.

Molecular Characterization

Several probe molecules of programme GRID (26) were employed to detect favourable non-covalent interactions with the ligands. Use of the alcoholic probes O1_{don} and O1_{acc} with hydrogen donor and hydrogen acceptor properties, respectively, yielded information about complementary features of the investigated molecules. For tracing hydrophobic interactions the DRY probe representing “hydrophobic water” was applied.

The SPARTAN software (27) was used to calculate solvation energies (AM1-aqueous method) and logP values according the Villar-AM1 algorithm. Furthermore, in order to investigate molecular electrostatic potentials (MEPs), ESP partial charges of the optimized structures were derived from the wave functions of restricted Hartree-Fock (RHF) ab initio calculations using the 6-31G** basis set.

All computations were carried out on SGI Origin2000, Indigo² R10000, SGI O2 R10000 and SGI Indy R4600 workstations.

RESULTS AND DISCUSSION

Sterical Pharmacophore Generation

For pharmacophore construction the rigid carbocyclic BOAs 5a–5f were used as references (Table III), since they comprise minimum requirements for specific BTZ binding. In order to determine energetically favourable arrangements of

ring B, the spiro-linked compound 5e as the most rigid derivative was subjected to a systematic conformational search yielding an optimum dihedral angle φ of -42° (Fig. 2a).

Subsequently, BTZ, BZ, PBTZ and P6Z derivatives were superimposed onto ring A of 5e and all conformations derived from the search procedure were screened (e.g., Fig. 2b) to find a common energetically favourable arrangement of all B rings. Furthermore, this analysis yielded low-energy conformers placing the ammonium functions almost identically when compared to the template (Fig. 3). For this sterical fit only 4'-methoxylated derivatives were used, since structure-affinity/activity relationships (SAR) of BZs reveal this particular substituent as being optimal (compare 2h–2l in Table I).

Molecular Characterization of the BTZ Pharmacophore Model

To explore essential molecular features of the preliminary sterical pharmacophore model and for characterizing potential non-covalent interactions with the binding site, hydrophobic (DRY) and alcoholic (O1_{don}/O1_{acc}) probe molecules of programme GRID (26) were employed. Application of the DRY probe (Fig. 4a) indicates favourable hydrophobic interactions parallel to the aromatic rings and close to the sulphur atom of BTZ, PBTZ and P6Z derivatives. With the O1_{don} probe a potential hydrogen bond acceptor region is observed that is connected with the free electron pairs of the 4'-ether oxygens (Fig. 4b). Comparison of BZs, which possess H-bond capacity (2h–2k) with the 4'-ethylated derivative 2l indicates this property to be more essential for calcium antagonism than for binding (Table I). On the other hand, lack of the terminal methyl group (i.e., 2i) leads to a pronounced loss of binding affinity, implicating both hydrogen bonding and hydrophobic contacts to be important for an accurate description of the ligand/receptor interaction.

Analysis of the fields obtained with O1_{acc} probe reveals a common potential hydrogen bond donor region at the protonated ammonium functions (Fig. 4b). By the same token, these cationic groups cause strong positive MEPs (Fig. 5). Therefore, hydrogen bonding and/or electronic forces might be involved in interactions with the binding site in this region. For BZ derivatives with structurally modified side chains, a remarkable decrease in activity is observed if the dimethylamine function (2g) is substituted against amide (2q), aldehyde (2r), hydroxyl (2s), or carboxylate (2t) moieties (see Table I). Although the negative charge of 2t at pH 7.4 (carboxylate anion) might prevent access to the lipophilic binding site, the neutral derivatives 2q and 2s should be able to reach their molecular targets. However no substantial difference is detected for these potential hydrogen donors (2q and 2s) compared to moieties, which lack this feature (2r). Furthermore, it was shown that in preparations of fragmented cell membranes receptor affinity of the quaternary BZ 2u differs only by a factor of eleven compared with the tertiary amine 2h (16). These findings indicate electrostatic forces rather than hydrogen bonding interactions as important features to stabilize the ammonium group at the binding site.

The carbonyl oxygens of BTZs and BZs induce strong negative potentials (Fig. 5). Interestingly, also the pyrrole rings of PBTZ and B6Z derivatives produce similar electrostatic fields, although their intensity is weaker. Besides the common

Table I. Experimental In Vitro Data of Racemic 1,4-Benzothiazepin-4(5*H*)-one (BTZ) and 1-Benzazepin-2-one (BZ) Derivatives

Compound	R ¹	R ²	R ³	IC ₅₀ ^a	K _d ^b
1a (diltiazem)	H	OCH ₃	—	1.8 (0.74–4.6)	0.38 (±0.04)
1b	Cl	OCH ₃	—	0.24 (0.16–0.38)	0.081 (±0.024)
1c	OCH ₃	OCH ₃	—	0.12 (0.072–0.19)	0.042 (±0.006)
2a	H	OCH ₃	OAc	4.7 (2.9–7.8)	5.1 (±1.4)
2b	7-Cl	OCH ₃	OAc	1.5 (0.84–2.8)	1.4 (±0.51)
2c	7-OCH ₃	OCH ₃	OAc	1.9 (0.88–4.0)	1.6 (±0.28)
2d	6-CH ₃	OCH ₃	OAc	2.5 (1.9–3.3)	n.d.
2e	6-CN	OCH ₃	OAc	0.12 (0.67–0.20)	n.d.
2f	6-NO ₂	OCH ₃	OAc	0.37 (0.24–0.58)	n.d.
2g	6-CF ₃	OCH ₃	OAc	0.15 (0.11–0.22)	0.12 (±0.018)
2h	6-CF ₃	OCH ₃	CH ₃	0.076 (0.041–0.14)	0.075 (±0.043)
2i	6-CF ₃	OH	CH ₃	0.16 (0.087–0.28)	1.6
2j	6-CF ₃	NHCH ₃	CH ₃	0.33 (0.20–0.56)	0.57 (±0.23)
2k	6-CF ₃	SCH ₃	CH ₃	0.73 (0.38–1.4)	1.1 (±0.40)
2l	6-CF ₃	CH ₂ CH ₃	CH ₃	2.4 (1.5–3.9)	1.0 (±0.20)
2m	6-CF ₃	OCH ₃	H	1.1 (0.75–1.7)	n.d.
2n	6-CF ₃	OCH ₃	CH ₂ CH ₃	0.012 (0.093–0.017)	0.60 (±0.17)
2o	6-CF ₃	OCH ₃	allyl	0.10 (0.064–0.17)	n.d.
Compound	X	Y	IC ₅₀ ^a	K _d ^b	
2p	CH ₂ N ⁺ H ₂ CH ₃	OAc	0.18 (0.12–0.28)	0.16 (±0.024)	
2q	CONHCH ₃	OAc	6.2 (3.7–10)	15 (±6.0)	
2r	CHO	OAc	>3	n.d.	
2s	CH ₂ OH	OAc	10 (6.5–15)	n.d.	
2t	COOH	OAc	>3	n.d.	
2u	CH ₂ N ⁺ (CH ₃) ₃	CH ₃	6.2 (4.9–7.9)	0.84 (±0.041)	

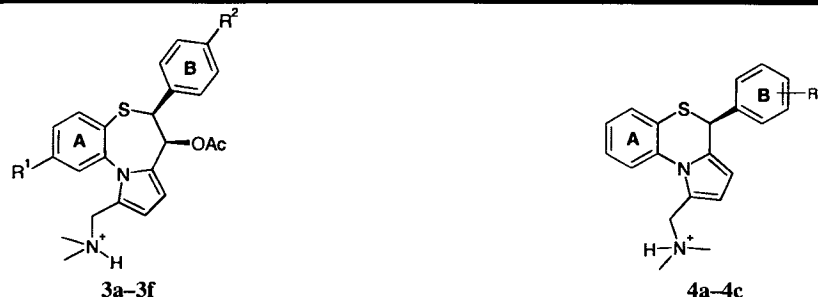
^a IC₅₀ (μM) in rabbit aorta strips contracted with KCl (95% confidence interval).

^b K_d in μM (±SEM), determined by displacement of radiolabeled diltiazem in guinea pig striated muscle. Experimental data taken from (15,16).

negative MEP along the 4'-ether oxygens, a further electron-rich region caused by the sulphur atom of all sulphur-containing BTZ-like derivatives is detected. The importance of this position becomes evident by comparing diltiazem (**1a**) with its analogous BZ derivative **2a**. The binding affinity of the sulphur-free BZ is diminished by more than one order of magnitude. However, higher binding affinities and stronger effects are achieved by insertion of hydrophobic substituents in 6- and 7-position of BZs (compare **2a** with **2b–2g**). A further increase in binding affinity is yielded for BZ derivatives of this series if the C6 substituents possess besides the hydrophobic characteristic also high electron density (compare **2d** with **2e–2g**). This implicates that hydrophobic and electron-rich features produced by the C6 substituents of BZs or the sulphur atom of BTZs are favourable for receptor binding.

On the other hand, it is surprising that the pyrrolo[2,1-*c*][1,4]benzoxazine derivative **6** (Table IV) shows such a dramatic decrease of affinity with respect to the B6Z analogue **4b**


(K_d 1750 vs. 0.16 nM). Following the above-mentioned findings, a sulphur-to-oxygen substitution should enhance the electronegative potential at this position and thereby yield compounds that are even more active. Since corresponding benzothiazine and benzoxazine derivatives have almost identical shapes and molecular geometries, this result can not be explained by modified spatial requirements. Therefore, in order to find an explanation for this finding, logP values and solvation energies (E_{sol}) were computed for the unprotonated compounds (Table IV). As expected, the benzoxazine derivative is less hydrophobic than the sulphur containing B6Z, but a difference of approximately one logP unit cannot alone account for four orders of magnitude difference in binding potencies (1:11,000). A more complete picture would be given by including the difference of 8.31 kcal/mol in solvation energies (see Table IV). In addition, a further aspect can be discussed in this context, namely the distinct electron distribution of the benzoxazine ring. Assuming that far-reaching electrostatic interactions between

Table II. Experimental in Vitro Data of Racemic Pyrrolo[2,1-*d*][1,5]benzothiazepine (PBTZ) and Pyrrolo[2,1-*c*][1,4]benzothiazine (P6Z) Derivatives


Compound	R ¹	R ²	IC ₅₀ ^a	K _i ^b
3a	H	H	5200 (±311)	2407 (±144)
3b	H	OCH ₃	136 (±68)	63 (±31)
3c	CF ₃	H	300 (±60)	139 (±28)
3d	CF ₃	OCH ₃	not active	n.d.
3e	Cl	H	1230 (±138)	569 (±64)
3f	Cl	OCH ₃	3.3 (±0.7)	1.5 (±0.213)
4a	—	H	315 (±60)	118 (±22.4)
4b	—	4'-OCH ₃	0.42 (±0.15)	0.16 (±0.06)
4c	—	2',4'-(OCH ₃) ₂	150 (±49.5)	56 (±18.6)

^a Necessary concentration (nM, ±SEM) to inhibit [³H]nitrendipine binding on rat cortex homogenate by 50% (diltiazem 46 (±6.5) nM).

^b Apparent inhibition constants (nM, ±SEM) calculated from the obtained IC₅₀ values by the Prusoff method (17); K_i diltiazem 21 (±2.9) nM. Experimental data taken from (18,19).

Table III. Experimental in Vitro Data of Benzobicyclo[2.2.2]octyl Amine (BOA) Derivatives


Compound	R ¹ /X	R ² /Y	IC ₅₀ ^a	K _d ^b
5a	H	N ⁺ H ₂ CH ₃	3.7 (2.6–5.3)	2.1 (±0.63)
5b	N ⁺ H ₂ CH ₃	H	4.2 (2.9–6.1)	0.89 (±0.20)
5c	H	CH ₂ N ⁺ H ₂ CH ₃	0.74 (0.49–1.1)	0.69 (±0.05)
5d	CH ₂ N ⁺ H ₂ CH ₃	H	0.87 (0.56–1.4)	0.60 (±0.02)
5e	N ⁺ H ₂	CH ₂	0.95 (0.76–1.2)	0.33 (±0.12)
5f	CH ₂	N ⁺ H ₂	2.0 (1.5–2.7)	1.3 (±0.28)

^a Necessary concentration (μM ±SEM) for a half-maximum relaxation of rabbit aorta strips contracted with KCl (95% confidence interval) [(+)-cis-diltiazem IC₅₀ 0.21 (0.13–0.36) μM].

^b Determined by displacement of radiolabeled diltiazem in guinea pig striated muscle in μM (±SEM) [(+)-cis-diltiazem K_d 0.20 (±0.02) μM]. Experimental data taken from (20).

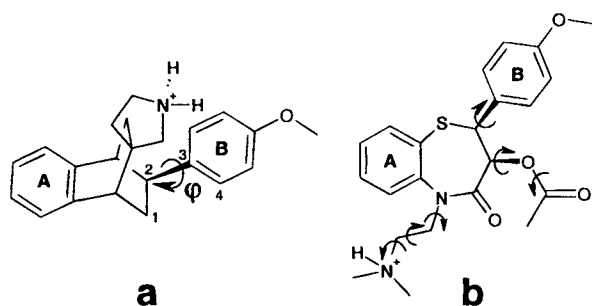


Fig. 2. Spiro-linked BOA 5e used as template for pharmacophore generation (a) in comparison to the classical BTZ derivative diltiazem (b). Fully rotated bonds for systematic conformational search and the aromatic rings A and B are indicated.

ligands and binding site are most important, the formal charge of the ammonium group might be the driving force for receptor approximation. Fine tuning at the binding cleft could occur via additional electrostatic contacts in combination with hydrophobic interactions. In this scenario, the most negatively charged regions of BTZ and BZ derivatives (carbonyl oxygens) might interact with the most electron-deficient site of the receptor. Therefore, the relative locations of electron-rich centres in the different molecules might be very important in understanding the variations in binding affinities. Also B6Z derivatives would fit into this scheme, since here the π-electrons of the aromatic pyrrole ring represent the electron-rich region. In the case of BTZs the sulphur atoms (or the electron-rich substituents of BZ derivatives) constitute a further however rather weak electrostatic interaction. If the hydrophobic sulphur atom of B6Zs

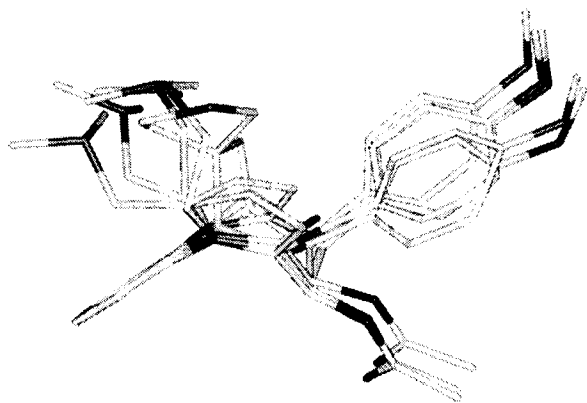


Fig. 3. Superposition of low-energy conformers of BTZ-like derivatives **1a**, **2a**, **3b**, **4b**, and **5e**. Nitrogen and oxygen atoms are highlighted (dark coloured) and hydrogens are not displayed.

is substituted against a hydrophilic oxygen atom (i.e., **6**), this position instead of the pyrrole π -system induces a stronger negative MEP. Consequently, the ligand has to flip in order to saturate the strongest positive potential of the binding site with the “false” oxygen counterpart. Although the ammonium side chain has enough flexibility to compensate this rotation, a correct receptor recognition of ring B would be prevented as in case of the d-cis- and l-cis-enantiomers of diltiazem (K_i 0.21 vs. 6.82 μM at 2°C) (28).

In order to prove the importance of the described electrostatic interactions, d-cis-diltiazem (**1a*** K_d 0.2 μM) and the BOA derivative **5e** (K_d 0.33 μM), which does not generate the MEPs necessary for this type of interaction, were compared. Taking into account that K_d values not only mirror direct ligand/

receptor interactions (i.e., vdW, electrostatic, hydrophobic, and H-bond contacts) but also changes of entropy (ΔS) and solvation energies, the latter two parameters were determined for both molecules. Considering an energy penalty of 0.8 kcal/mol per rotatable bond if the ligand is bound at the receptor site (29,30), binding affinity of diltiazem (7 relevant rotatable bonds) should be about 4 kcal/mol lower compared with the affinity of **5e** (2 relevant rotatable bonds). Obviously, this term may not explain higher receptor affinity of diltiazem. Subsequently, solvation energies (E_{solv}) and logP values were computed based on the semiempirical AM1 method. Also these calculations reveal a preference of **5e** over **1a** to reach the intramembraneous binding site (see Table IV).

Summarizing these findings, the BOA derivative but not diltiazem should exert higher binding affinity implicating the necessity of diltiazem to interact via additional direct contacts (probably induced by the above discussed negative MEPs) with the receptor site to overrule its “unfavourable” physico-chemical parameters.

Influence of Substituents in 3-Position of BTZ and BZ Derivatives

Concerning 3-acetoxy substituted BTZ (**1a–1c**) or BZ derivatives (e.g., **2a–2g**), also the ester oxygens can act as potential hydrogen bond acceptors (Fig. 4) and induce pronounced negative MEPs (Fig. 5). However, substitution of acetoxy (**2g**) against methyl (**2h**), ethyl (**2n**) or allyl (**2o**) moieties even enhances activity and binding affinity of BZs, whereas removal of any substituent leads to a pronounced loss of activity (**2m**). This clarifies that the presence rather than the chemical nature of a substituent is crucial.

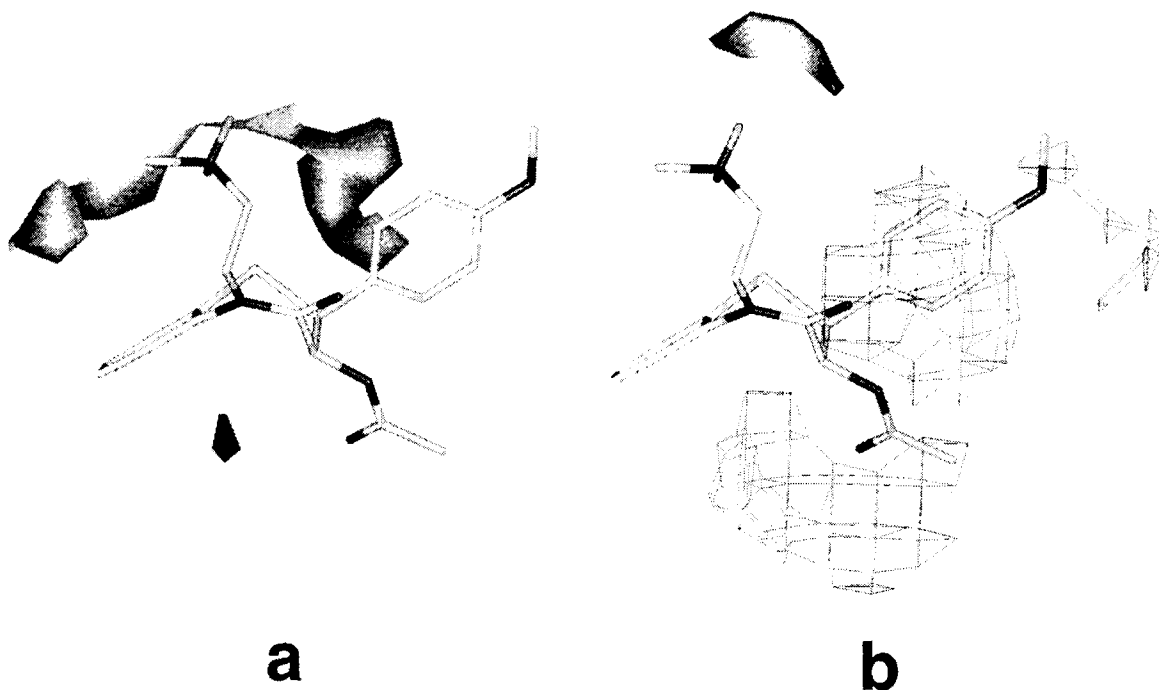


Fig. 4. Diltiazem (**1a**) with fields derived from use of the GRID programme (26). a: Potential hydrophobic regions (cloud) contoured at -0.7 kcal/mol. b: The cloud indicates a potential hydrogen accepting area of the binding site contoured at -3.0 kcal/mol. Grid fields depict hydrogen donor regions contoured at -3.5 kcal/mol.

Table IV. Comparison of Experimental Binding Data with Computationally Derived Parameters for Pyrrolo[2,1-c][1,4]benzothiazine, Pyrrolo[2,1-c][1,4]benzoxazine, 1,4-Benzothiazepin-4(5H)-one and Benzobicyclo[2.2.2]octyl Amine Derivatives

Compound	IC ₅₀ ^a	K _d ^b	logP ^c	E _{solv.} ^d
4b	0.42	0.16	5.37	-17.23
6	4670	1750	4.58	-25.54
1a*	0.21	0.20	2.91 [§]	-27.86
5e	0.95	0.33	4.04	-21.65

^a Concentration (nM) necessary to inhibit [³H]nitrendipine binding on rat cortex homogenate by 50%.

^b Apparent inhibition constants (nM) calculated from the IC₅₀ values according to the Prusoff method (17). Experimental data are taken from (19).

^c Calculated applying the Villar-AM1 algorithm implemented in the SPARTAN software package (27).[§] The measured logP of diltiazem is 2.7.

^d Calculated with the AM1-Aq method of SPARTAN (27) [kcal/mol]. **1a*** is d-(cis)-diltiazem.

In order to examine the contribution of a 3-substituent to the spatial orientation of ring B a comparative study of the 3-methyl BZ derivative **2h** and the non-substituted BZ **2m** (3-H) was carried out. In course of this investigation the C4-C1' bond (φ) was fully rotated in both molecules and the corresponding potential energies were compared. The resulting energy curves (Fig. 6a) show two identical global minima for each compound ($\varphi = 110^\circ$ and 290°). For the unsubstituted BZ **2m** three additional local minima are found with $\Delta E_{\text{pot}} \approx 4$ kcal/mol over the global minimum.

In a second approach, molecular dynamics simulations (mds) at different temperatures were performed to explore the special role of the 3-methyl substituent for a stabilization of the bioactive "M" twist-boat conformation.

The results derived from these simulations (Fig. 6b) reveal that at 800 K and 900 K the 7-membered ring of **2m** (3-H) undergoes transition from the bioactive "M" twist-boat ($\phi \approx -110^\circ$) to an inverted boat conformation $\phi \approx -120^\circ$. But only at 900 K the temperature is sufficient to surmount the energy barrier for a reversion into the initial conformation. In contrast, the heptagonal ring of **2h** (3-CH₃) remains almost exclusively in the bioactive conformation even at the highest chosen temperature of 900 K.

Subsequently, a simulated annealing procedure was carried out using the proposed bioactive conformers as well as the inverted boat conformations of **2m** and **2h** as input structures. Analysis of the archived frames (at 0 K) indicated that independent of the chosen input structure transitions between both

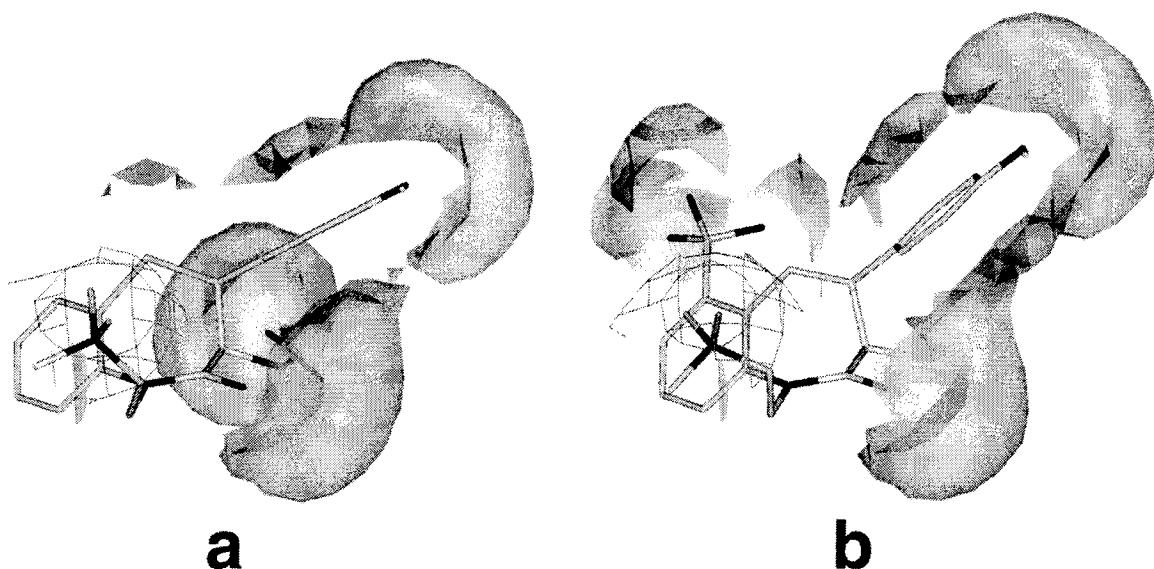


Fig. 5. Top view of diltiazem (a) and the BZ derivative **2h** (b). Positively charged regions are contoured at a level of +60 kcal/mol (grids) and negative MEPs are indicated as transparent clouds at -0.7 kcal/mol.

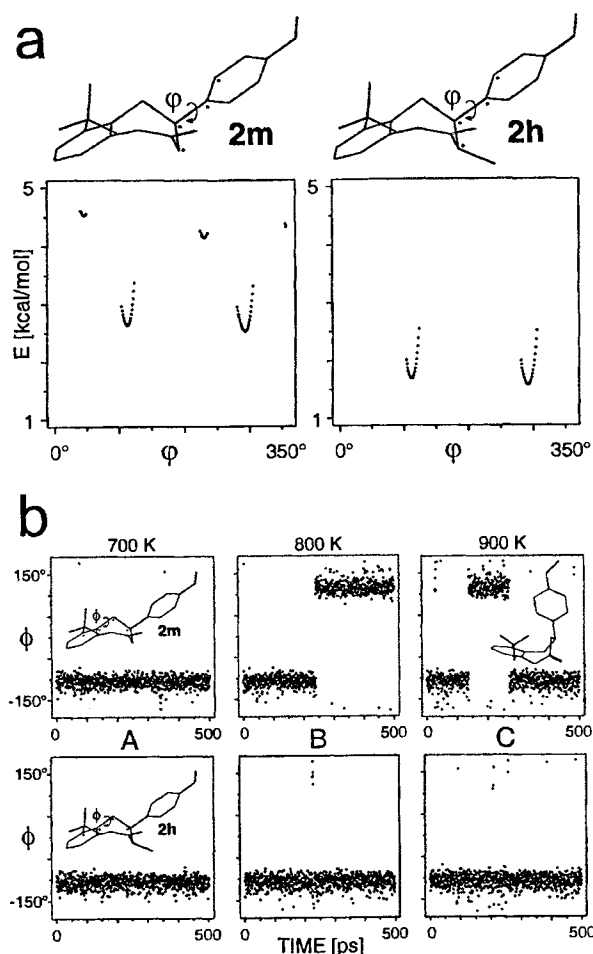


Fig. 6. Comparative investigations of the BZ derivatives **2m** and **2h** (for clarity the basic side chains are undisplayed). a: Energy curves (SYBYL systematic search) for the 3-unsubstituted BZ_{2m} and the 3-methylated derivative **2h**. b: Results derived from molecular dynamics simulations. Each graph shows the variation of the dihedral angle (ϕ) measured along the four atoms marked in the starting conformations of **2m** and **2h** (see inlays of graphs A) in the course of 500 ps simulations at 700 K (A), 800 K (B) and 900 K (C). Each rhombus at $\phi \approx -110^\circ$ represents one conformer with an almost unaltered “M” twist-boat conformation of the heptagonal ring. For **2m** transitions to inverted boat conformations $\phi \approx 120^\circ$ (see inlay of graph C) are detected at 800 K and 900 K, whereas **2h** remains almost exclusively in the starting conformation.

arrangements are possible. The ratio between both forms, however, is affected by the 3-substituent yielding a preference for the bioactive conformation of **2h** (60%) compared with derivative **2m** (35%). Closer examination of the individual conformers reveals an energetic difference of only 1.7 kcal/mol between the minimized boat and inverted boat form of **2m** whereas the bioactive conformation of **2h** is 7.0 kcal/mol more favourable with respect to the inverted boat form.

These results demonstrate the stabilizing effects of substituents in 3-position on the bioactive conformation of the benzazepinone ring. In addition, they restrict the rotational flexibility of ring B leading to a loss of entropy and thereby ease binding of the ligands to the receptor.

In agreement with earlier findings (16,18–20,31) our work yields a pharmacophore model for BTZ-like derivatives comprised of three crucial features, (i) two aromatic ring systems (ring A and B) in a distance of about 6.7 Å, (ii) a basic centre with $pK_a \approx 7.4$ pointing in the same direction as ring B, and (iii) a 4'-methoxy substituent at ring B. Further pharmacophoric elements which favour binding and calcium antagonistic effect, are (i) a strong negative MEP in 4-position of BTZ/BZ derivatives, (ii) a hydrophobic electron-rich region in the position equivalent to the sulphur atom of BTZs, and (iii) a substituent in 3-position of benzepine rings.

Proposal of the Quinazolinone Derivative MCI-176 as Potential Diltiazem Mimic

A multitude of diverse drugs and toxins modulate L-type calcium channels via distinct mechanisms (2,32). This finding indicates that calcium entry blocking activity is not strictly coupled to closely related chemical structures. However assuming one common binding site for various modulators their pharmacological profiles should be comparable even if the ligands are structurally diverse. Since diltiazem-like effects have been reported for the quinazolinone calcium channel blocker MCI-176 (33–35), we investigated the properties of this compound (Fig. 7) in comparison with the BTZ derivative **1c** in order to proof its potential to behave as a ligand of the BTZ binding site.

In accordance with the procedure described above, all energetically accessible conformations of MCI-176 obtained from conformational analyses were probed to satisfy the pharmacophoric features. Hereby, special attention was directed towards the fulfilment of the three absolutely crucial pharmacophoric requirements of BTZ-like derivatives. Especially the 4'-methoxy group of ring B seemed to be critical, although MCI-176 has two methoxy groups, however in 2'- and 5'-position.

Analysis of the search results yielded several low energy conformers of **1c** (Fig. 7) that perfectly fit the proposed bioactive conformer of **1c** (Fig. 7). The superposition indicates ammonium groups and aromatic rings (A and B) in almost identical positions. Interestingly, one of the two methoxy groups of MCI-176 takes the role of the 4'-methoxy rest of the reference structure. Also with respect to electronic features the similarity between the compared structures is remarkable since the expected strong positive MEPs in the environment of the ammonium

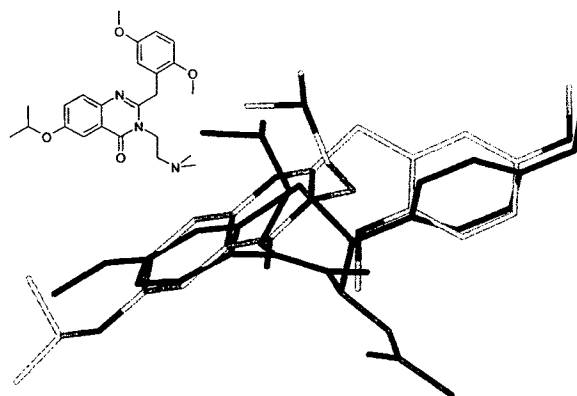


Fig. 7. Structural formula of the calcium channel blocking quinazolinone derivative MCI-176 and superposition of MCI-176 (grey) onto the most active BTZ derivative **1c** (black).

group and also the characteristic negative potential induced by carbonyl oxygen at C4 are found in equivalent locations. Even an equivalent for the negative field induced by the sulphur of BTZs exists in MCI-176 and the large isopropoxy group might act by substituting for lipophilic residues like chlorine as found for example in 3f (see Table II).

Summarizing the results of this comparison, we predict the quinazolinone derivative MCI-176 to behave as a BTZ-like ligand at the diltiazem binding site of L-type calcium channels.

ACKNOWLEDGMENTS

We are grateful to Prof. Dr. H.-D. Höltje, Heinrich-Heine-University Düsseldorf, for constructive discussions and for providing all hard- and software facilities.

REFERENCES

1. D. Rampe and D. J. Triggle. New ligands for L-type Ca^{2+} channels. *Trends Pharmacol. Sci.* **11**:112–115 (1990).
2. H. Glossmann and J. Striessnig. Molecular properties of calcium channels. *Rev. Physiol. Biochem. Pharmacol.* **114**:1–105 (1990).
3. J. Striessnig, M. Grabner, J. Mitterdorfer, S. Hering, M. J. Sinnegger, and H. Glossmann. Structural basis of drug binding to L Ca^{2+} channels. *Trends Pharmacol. Sci.* **19**:108–115 (1998).
4. E. Anselmi, G. Fayos, R. Blasco, L. Candenias, D. Cortes, and M. P. D'Ocon. Selective inhibition of calcium entry induced by benzylisoquinolines in rat smooth muscle. *J. Pharm. Pharmacol.* **44**:337–343 (1992).
5. D. Cortes, M. Y. Torrero, M. P. D'Ocon, M. L. Candenias, A. Cavé, and A. H. A. Hadi. Norstephalagine et atherospermidine, deux aporphines d'artabotrys maingayi relaxantes du muscle lisse. *J. Nat. Prod.* **53**:503–508 (1990).
6. M. D. Ivorra, C. Lugnier, C. Schott, M. Catret, M. A. Noguera, E. Anselmi, and M. P. D'Ocon. Multiple actions of glaucine on cyclic nucleotide phosphodiesterases, α_1 -adrenoceptor and benzothiazepine binding site at calcium channel. *Br. J. Pharmacol.* **106**:387–394 (1992).
7. M. D. Ivorra, S. Chuliá, C. Lugnier, and M. P. D'Ocon. Selective action of two aporphines at α_1 -adrenoceptors and potential-operated Ca^{2+} channels. *Eur. J. Pharmacol.* **231**:165–174 (1993).
8. R. A. Sheehan-Dare and M. J. D. Goodfield. Widespread cutaneous vasculitis associated with diltiazem. *Postgrad. Med. J.* **64**:467–468 (1988).
9. M. Lahav and R. Arav. Diltiazem and thrombocytopenia. *Ann. Int. Med.* **110**:327 (1989).
10. P. C. Waller and W. H. W. Inman. Diltiazem and heart block. *Lancet* **1**:617 (1989).
11. R. S. Dick and S. S. Barold. Diltiazem-induced parkinsonism. *Am. J. Med.* **87**:95–96 (1989).
12. H. Shallcross, S. P. G. Padley, M. J. Glynn, and D. D. Gibbs. Fatal renal and hepatic toxicity after treatment with diltiazem. *Br. Med. J.* **295**:1236–1237 (1987).
13. Cambridge Structural Database, Cambridge Crystallographic Data Center, Cambridge, U.K.
14. F. H. Allen, O. Kennard, and D. G. Watson. Crystallographic databases: Search and retrieval information from the Cambridge Structural Database. *Struct. Correl.* **1**:71–110 (1994).
15. D. M. Floyd, S. D. Kimball, J. Krapcho, J. Das, C. F. Turk, R. V. Moquin, M. W. Lago, K. J. Duff, V. G. Lee, R. E. White, R. E. Ridgewell, S. Moreland, R. J. Brittain, D. E. Normandin, S. A. Hedberg, and G. G. Cucinotta. Benzazepinone calcium channel blockers. 2. Structure-activity and drug metabolism studies leading to potent antihypertensive agents. Comparison with benzothiazepines. *J. Med. Chem.* **35**:756–772 (1992).
16. S. D. Kimball, D. M. Floyd, J. Das, J. T. Hunt, J. Krapcho, G. Rovnyak, K. J. Duff, V. G. Lee, R. V. Moquin, C. F. Turk, S. A. Hedberg, S. Moreland, R. J. Brittain, D. M. McMullen, D. E. Normandin, and G. G. Cucinotta. Benzazepinone calcium channel blockers. 4. Structure-activity overview and intracellular binding site. *J. Med. Chem.* **35**:780–793 (1992).
17. Y. Cheng and W. H. Prusoff. Relationship between the inhibition constant (K_1) and the concentration of inhibitor which causes 50 per cent inhibition (I50) of an enzymatic reaction. *Biochem. Pharmacol.* **22**:3099–3108 (1973).
18. G. Campiani, I. Fiorini, M. P. De Filippis, S. M. Ciani, A. Garofalo, V. Nacci, G. Giorgi, A. Segal, M. Botta, A. Chiarini, R. Budriesi, G. Bruni, M. R. Romeo, C. Manzoni, and T. Menzini. Cardiovascular characterization of pyrrolo[2, 1-d][1, 5]benzothiazepine derivatives binding selectively to the peripheral-type benzodiazepine receptor (PBR): From dual PBR affinity and calcium antagonist activity to novel and selective calcium entry blockers. *J. Med. Chem.* **39**:2922–2938 (1996).
19. G. Campiani, A. Garofalo, I. Fiorini, M. Botta, V. Nacci, A. Tafi, A. Chiarini, R. Budriesi, G. Bruni, and M. R. Romeo. Pyrrolo[2, 1-c][1, 4]benzothiazines: Synthesis, structure-activity relationships, molecular modeling studies, and cardiovascular activity. *J. Med. Chem.* **38**:4393–4410 (1995).
20. J. C. Barrish, S. H. Spergel, S. Moreland, G. Grover, S. A. Hedberg, A. T. Pudzianowski, J. Z. Gougoutas, and M. F. Malley. Conformationally constrained calcium channel blockers: Novel mimics of 1-benzazepin-2-ones. *Bioorg. Med. Chem.* **1**:309–325 (1993).
21. SYBYL v. 6.5, Tripos Associates, Inc., St. Louis, MO, U.S.A.
22. D. J. Mazzo, C. L. Obetz, and J. Shuster. Diltiazem hydrochloride. *Anal. Profiles Drug Subst. Excipients* **23**:53–98 (1994).
23. IXGROS, part of Ph.D. Thesis, Sippl, W., Düsseldorf, Germany, 1997.
24. M. J. S. Dewar, E. G. Zebisch, E. F. Healy, and J. J. P. Stewart. AM1: A new general purpose quantum mechanical molecular model. *J. Am. Chem. Soc.* **107**:3902–3909 (1985).
25. T. A. Halgren. Merck molecular force field. I. Basis, form, scope, parameterization, and performance of MMFF94*. *J. Comput. Chem.* **17**:490–519 (1996).
26. GRID, v. 16, Molecular Discovery Ltd., Oxford, U.K.
27. SPARTAN 4.1.1, Wavefunction, Irvine, CA, U.S.A.
28. S. Ikeda, J.-I. Oka, and T. Nagao. Effects of four diltiazem stereoisomers on binding of d-cis-[^3H]diltiazem and (+)-[^3H]PN200-110 to rabbit T-tubule calcium channels. *Eur. J. Pharmacol.* **208**:199–205 (1991).
29. M. S. Searle and D. H. Williams. The cost of conformational order: Entropy changes in molecular associations. *J. Am. Chem. Soc.* **11**:10690–10697 (1992).
30. A. J. Doig and D. H. Williams. Binding energy of an amide-amide hydrogen bond in aqueous and nonpolar solvents. *J. Am. Chem. Soc.* **114**:338–343 (1992).
31. V. Kettmann and H.-D. Höltje. Mapping of the benzothiazepine binding site on the calcium channel. *Quant. Struct.-Act. Relat.* **17**:91–101 (1998).
32. G. W. Zamponi. Antagonist binding sites of voltage-dependent calcium channels. *Drug Dev. Res.* **42**:131–143 (1997).
33. D. Horii and A. Ishibashi. Coronary dilator effect of MCI-176, a new calcium channel blocker, in dogs. *Tohoku J. Exp. Med.* **150**:101–102 (1986).
34. A. Ishibashi and D. Horii. Effect of MCI-176, a new calcium antagonist, on the calcium induced contraction of isolated porcine coronary arteries. *Jpn. J. Pharmacol.* **43**:234–236 (1987).
35. T. Ishibashi, M. Nakazawa, and S. Imai. Effect of MCI-176, a new calcium channel blocker, on large and small coronary arteries in dogs. *Cardiovasc. Res.* **23**:295–302 (1989).